Supramolecular Chemistry
Publication details, including instructions for authors and subscription information:
http://www.informaworld.com/smpp/title~content=t713649759

Modelling the response function of enzyme-based optical glucose-sensing capsules

Koji Tohda[a]; Tatsuya Yamamoto[a]; Miklós Gratzl[b]
[a] Graduate School of Science and Engineering for Research, University of Toyama, Toyama City, Toyama, Japan [b] Department of Biomedical Engineering, CASE (Case Western Reserve University), Cleveland, OH, USA

Online publication date: 23 June 2010

To cite this Article Tohda, Koji , Yamamoto, Tatsuya and Gratzl, Miklós(2010) 'Modelling the response function of enzyme-based optical glucose-sensing capsules', Supramolecular Chemistry, 22: 7, 425 — 433
To link to this Article: DOI: 10.1080/10610278.2010.483734
URL: http://dx.doi.org/10.1080/10610278.2010.483734

Supramolecular Chemistry
Vol. 22, Nos. 7–8, July–August 2010, 425–433

Taylor & Francis
Taylor & Francis Group

Modelling the response function of enzyme-based optical glucose-sensing capsules

Koji Tohda[a]*, Tatsuya Yamamoto[a] and Miklós Gratzl[b]

[a]*Graduate School of Science and Engineering for Research, University of Toyama, 3190 Gofuku, Toyama City, Toyama 930-8555, Japan;* [b]*Department of Biomedical Engineering, CASE (Case Western Reserve University), Cleveland, OH 44106, USA*

(*Received 15 January 2010; final version received 26 March 2010*)

A theoretical model for submillimetre-sized optical glucose sensors based on microscopic pH-sensitive optode beads and glucose oxidase (GOX) inside hydrophilic membrane capsules with ca. 12 μm thickness is presented. In this model, glucose influx and gluconic acid efflux across the capsule membrane are combined with enzymatic kinetics inside the capsule. Thereby, a simple model predicting the sensor responses with different permeabilities of the capsule membranes is obtained. The permeability of the capsule membranes for glucose and gluconic acid was successfully modified by changing the monomer ratio between 2-hydroxyethyl methacrylate (HEMA) and polyethylene glycol methacrylate (PEGMA) in the preparation of poly(HEMA-co-PEGMA)-based capsule membranes. Excellent agreements between the predicted sensor responses and the experimentally obtained ones were achieved in buffer solutions containing glucose at physiologically relevant concentrations. Consequently, this model can predict enhancement of the sensor response for glucose by reducing the gluconic acid efflux, and provides a general precept for the fabrication of enzyme-based optical sensors with enhanced responses.

Keywords: enzyme biosensor; response model; optode; diffusion coefficient; hydrogel

Introduction

In vivo monitoring of glucose has been one of the major objectives of academic and clinical research for many decades (*1–3*). This is especially true in the case of diabetics; tight glucose control facilitated by an implantable, continuous glucose sensor could greatly reduce the complications of diabetes, namely retinopathy, nephropathy, neuropathy and cardiovascular problems. Various approaches are under investigation or have been studied to achieve continuous monitoring in a reliable fashion using optical and electrochemical glucose sensors (*4–9*).

Enzyme-based electrochemical sensors are used in many fields of analytical chemistry for the quantification and monitoring of different biological and chemical compounds (*10*, *11*). For the quantification of glucose, glucose oxidase (GOX)-based electrochemical sensors comprising a frequently studied class of biosensors for *in vivo* application are used because of the relatively high durability, specificity and accuracy of the enzyme-based system, and high practical relevance of glucose measurements. Several papers have been published so far, describing the theoretical considerations about the kinetic response properties of their GOX-based electrochemical sensors, including electrochemically mediated ones (i.e. second-generation sensors) and enzyme-direct electron transfer ones (i.e. third-generation sensors) (*12–19*).

Optical glucose sensing is an alternative methodology for *in vivo* monitoring of glucose with an inherent safety advantage over the electrochemical sensors – no electrical connection to the patient's body is involved. Recently, McShane et al. reported optical glucose microsensor systems based on the encapsulation of an enzyme assay within the hydrogel microspheres (*20–22*). These sensors show fluorescent responses to glucose via change in oxygen concentration due to an enzymatic reaction by a fluorescent oxygen indicator co-encapsulated with the enzyme. Their intended application is as implantable devices for interstitial glucose monitoring in persons with diabetes; the sensors would be implanted intradermally and interrogated transdermally using light. A mathematical model of fluorescence-based optical-sensing microspheres has also been investigated (*20*, *22*).

We recently reported a submillimetre-sized array of sensing capsules for optical monitoring of pH, potassium and glucose designed for *in vivo* applications (*23–25*). For the glucose sensor, GOX-immobilised microscopic beads were stuffed into a microcapsule together with pH-sensitive optical microscopic beads. Glucose was monitored as the change in the colour of the glucose sensor due to the change in the local pH inside the sensing capsule, which is induced by the generation of gluconic acid as a result of the enzymatic reaction. Hundreds of glucose-sensing capsules with the same composition were fabricated to ensure the reproducibility of the optical

*Corresponding author. Email: tohda@eng.u-toyama.ac.jp

ISSN 1061-0278 print/ISSN 1029-0478 online

DOI: 10.1080/10610278.2010.483734
http://www.informaworld.com

glucose response. Among them, around 80% of the sensing capsules showed excellent colour response for glucose in the physiologically relevant concentration region. However, the other sensing capsules lost the potential for glucose response entirely; tiny cracks or holes in the capsule membranes of all the defective sensing capsules were observed under a microscope. This result suggests that the capsule membrane plays an indispensable role in optical glucose response by means of regulating the diffusion of glucose and gluconic acid across the membrane. It was also found that, by reducing the permeability of gluconic acid across the capsule membranes, the sensing capsule was able to attain an enhanced colour response. However, both a predictive model describing the response function of such sensors and the correlation of the said model to the experimental results have not been reported so far.

In this study, optical glucose sensors based on microscopic pH-sensitive optical beads and GOX entrapped inside the hydrophilic membrane capsules have been fabricated. A theoretical model describing the sensor response function based on the enzymatic kinetics and diffusion across the capsule membranes was developed and experimentally verified for the optical glucose-sensing capsules with different permeabilities of the capsule membranes.

Experimental

Reagents and chemicals

2-Hydroxyethyl methacrylate monomer (HEMA), di(ethylene glycol)dimethacrylate (DEGDMA), acrylamide and *N,N′*-methylene-bis-acrylamide were purchased from Tokyo Chemical Industry (Tokyo, Japan) and used without purification. Poly(ethylene glycol) (PEG: MW 600), GOX (EC 1.1.3.4 from *Aspergillus niger*) with a specific activity of 150–250/mg of solid and D(+)-glucose were purchased from Wako Laboratory Chemicals (Osaka, Japan). PEG methacrylate (PEGMA, average M_n ca. 360) was purchased from Aldrich (St Louis, MO, USA). Photoinitiators, 2,2-dimethoxy-1,2-diphenylethan-1-one (Irgacure 651) and 2-hydroxy-1-[4-(2-hydroxyethoxy)phenyl]-2-methyl-1-propanone (Irgacure 2959), were obtained from Ciba Specialty Chemicals, Inc. (Tarrytown, NY, USA) as gifts. Hydrogen ion selective chromoionophore III (9-diethylamino-5-[(2-octyldecyl)imino]benzo[a]phenoxazine), sodium tetrakis[3,5-bis(1,1,1,3,3,3-hexafluoro-2-methoxy-2-propyl)phenyl]borate (NaHFPB), bis(2-ethylhexyl)sebacate (BEHS) and poly(vinyl chloride) (PVC) were purchased from Fluka (Milwaukee, WI, USA) and used without purification. Bis[(12-crown-4)methyl]-2-dodecyl-2-methylmalonate (bis(12-crown-4)) was obtained from Dojindo Laboratories (Kumamoto, Japan). All the other reagents were of analytical reagent grade and used without further purification.

Calibration solutions were prepared from phosphate buffered saline (PBS) with a pH of 7.4 at 25°C (Wako) containing 138 mM of NaCl, 2.7 mM of KCl, 8.3 mM of Na_2HPO_4 and 1.4 mM of KH_2PO_4. Deionised water (specific resistance $> 18.2\,M\Omega$ cm) obtained using a Milli-Q water system (Millipore Corp., Bedford, MA, USA) was used in all solutions.

Procedures

Preparation of microscopic-sensing beads

PVC/BEHS beads: Microscopic beads based on 50 wt% of PVC and 50 wt% of BEHS with an average diameter of $2.5 \pm 1.0\,\mu m$ were prepared using a spray dry method, which has been reported elsewhere (*24*).

pH/Na^+-sensing microscopic beads: To 150 mg of the PVC/BEHS beads, 25 mg of BEHS solution containing 0.3 mg of hydrogen ion sensitive chromoinophore III, 0.96 mg of NaHFPB and 6.12 mg of sodium ionophore, bis(12-crown-4), were added and thoroughly mixed.

Beads mixture for glucose sensing: To prevent curdling of the sensing beads, the beads were suspended and fixed with hydrogel matrix. Two milligrams of the pH/Na^+-sensing beads were mixed well with 3 mg of PEG, 2 mg of GOX and 2 mg of an aqueous monomer solution containing 30 wt% of acrylamide, 1 wt% of *N,N′*-methylene-bis-acrylamide and 0.5 wt% of Irgacure 2959. The dispersed mixture was placed in between two slide glasses and then photopolymerised upon UV light irradiation for 15 min (low-intensity 365 nm UV light (Spectroline Pencil longwave UV lamp with $2\,mW/cm^2$ relative intensity at 1″); Fisher Scientific, Pittsburgh, PA, USA).

Fabrication of a micro-miniature poly(HEMA-co-PEGMA)-based sensor

A monomer solution of 80 wt% HEMA, 8.0 wt% PEGMA, 2.0 wt% DEGDMA, 9.8 wt% deionised water and 0.2 wt% Irgacure 651 was transferred into a mould consisting of two surface-modified slide glasses with octadecylsilane (26×76 mm) separated by a spacer with $200\,\mu m$ thickness (Figure 1(A)). The solution was polymerised to form a cross-linked hydrogel by exposure to low-intensity 365 nm UV light for 10 min. After polymerisation, the thus prepared polymer plate was cut into half using scissors. To prepare a well in the plate for a sensor body, one piece of the plate was punctured using an injection needle with a flat end but a sharp edge ($500\,\mu m$ diameter; Figure 1(B)). To seal the bottom of the punctured sensor body, $10\,\mu l$ of the above-mentioned monomer solution was applied to the surface of the other piece of the plate on the slide glass and spread. The punctured plate was placed on the monomer-applied plate, covered with a slide glass and clamped with binder clips (Figure 1(C)). After exposing to UV light for

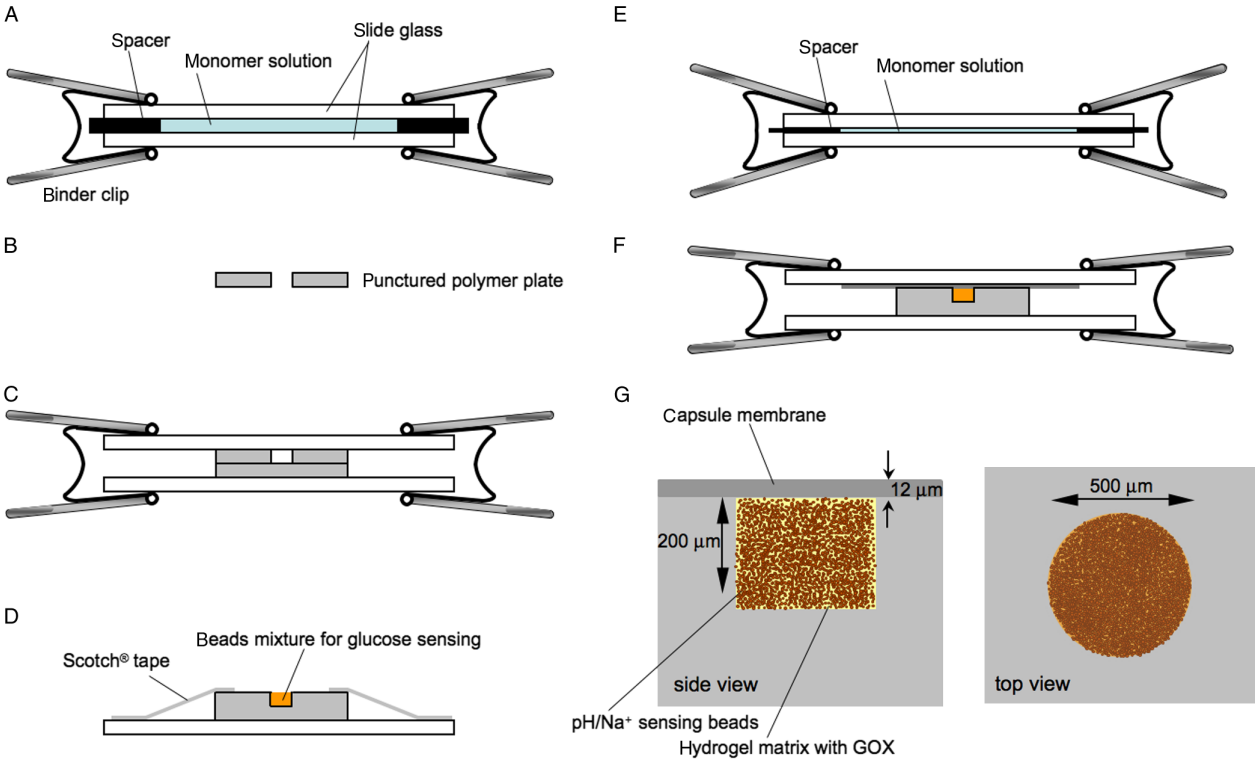

Figure 1. Preparation scheme for a submillimetre-sized optical-sensing capsule: (A) a monomer solution is transferred into a mould consisting of two slide glasses separated by a spacer with 200 µm thickness; (B) after polymerisation, the thus obtained polymer plate is punctured using an injection needle (500 µm diameter); (C) the bottom of the punctured polymer plate is sealed with the other piece of the polymer plate by photopolymerisation; (D) the beads mixture for glucose sensing is stuffed into the well of the sensor body; (E) to prepare the sensor capsule membrane, a monomer solution is transferred into a mould consisting of two slide glasses separated by a spacer with 12 µm thickness and then photopolymerised; (F) the sensor body stuffed with sensing beads mixture is sealed with the capsule membrane by photopolymerisation and (G) finally, a submillimetre-sized optical-sensing capsule is fabricated.

10 min, a poly(HEMA-co-PEGMA)-based sensor body containing a well with a sealed bottom was successfully prepared.

The thus prepared sensor body was placed on a slide glass with the sealed bottom down and fixed with pieces of Scotch® tape at the edges of the sensor body. The beads mixture for glucose sensing was stuffed into the well of the sensor body using a tiny glass rod under a stereomicroscope (Figure 1(D)).

To prepare the sensor capsule membrane, a monomer solution containing 30.0–45.0 wt% HEMA, 20.0–5.0 wt% PEGMA, 49.8 wt% deionised water and 0.2 wt% Irgacure 651 was put into a mould consisting of two slide glasses having hydrophobic surfaces separated by a spacer with 12 µm thickness (Figure 1(E)). After polymerisation by exposure to UV light for 12 min, one of the slide glasses in the mould was carefully removed. In doing so, the polymer capsule membrane with 12 µm thickness remained on the surface of the other slide glass. To adhere the sensor body with this capsule membrane, 10 µl of the above-mentioned monomer solution was applied to the surface of the thus prepared capsule membrane on the slide glass and spread. The sensor body was then placed on the capsule membrane, covered with a slide glass and clamped with binder clips (Figure 1(F)). By exposing to UV light for 6 min, a well with beads mixture in the sensor body was successfully sealed with a thin capsule membrane. A schematic diagram of the thus prepared glucose-sensing capsule is shown in Figure 1(G).

Apparatus and data acquisition

A flow-through cell made of polyacetal resin with a single glass window was used to monitor the sensor colour response. The volume of the chamber in the flow-through cell was around 200 mm^3. A sensing capsule was adhered onto the bottom of the chamber in the flow-through cell with silicone glue. A PBS solution was then pumped through the cell at 1 ml/min (linear flow rate: ~10 cm/min) with a peristaltic pump for conditioning for 2 h. Glucose concentrations were then varied by switching the pump to the respective solutions. The measurements were carried out at room temperature.

Each measurement consisted of taking a captured image with a charge coupled device (CCD) camera-based microscope system without gamma correction (Video

Zoom Microscope 1000 colour system, Edmund Industrial Optics, Dunedin, FL, USA). A halogen lamp illuminator with a fibre optic ring light guide was used as a light source. Mathematica 5.2 (Wolfram Research, Inc., Champaign, IL, USA) was used for image analyses.

Theory

The enzyme kinetics inside a sensing capsule coupled with the flux of glucose and gluconic acid across the capsule membrane provides the basis of the theoretical model. Glucose detection depends on the change in local pH inside the sensing capsule as a result of the generation of gluconic acid with the enzymatic reaction. Thus, the concentration of gluconic acid has to be included in the mathematical treatment for predicting the sensor response. Figure 2 shows a schematic representation of the sensor response model with three steps of kinetics: (1) influx of glucose across the capsule membrane, (2) generation of gluconic acid by the enzymatic reaction of GOX with glucose inside the sensing capsule and (3) efflux of gluconic acid across the capsule membrane. In order to simplify the theoretical treatment, we set the concentration of glucose inside the sensing capsules lower than that of oxygen, so that the enzyme reaction is glucose limited. It is assumed that the rate-determining step of the sensor response is the diffusion across the capsule membrane. This means that the concentrations of glucose and gluconic acid are homogeneous both inside and outside the sensing capsule; only within the capsule membrane do the concentration gradients exist. The capsule membrane is assumed to be homogeneous and isotropic such that the permeability is governed by diffusivity of glucose and gluconic acid.

Influx of glucose across the capsule membrane

To describe the influx of glucose across the capsule membrane, Fick's law for planar diffusion can be used, because the sensor has a planar capsule membrane whose thickness, i.e. diffusion thickness, is much lesser than the sensor diameter (Figure 1(G)). Accordingly,

$$J_{S(t)} = -D_S \frac{\partial C_S}{\partial x} = D_S \frac{C_S^0 - C_{S(t)}}{l}, \quad (1)$$

where $J_{S(t)}$ is the influx of glucose at time t, D_S is the diffusivity of glucose in the capsule membrane, C_S^0 is the concentration of bulk glucose outside the sensing capsule, $C_{S(t)}$ is the concentration inside the sensing capsule and l is the thickness of the capsule membrane.

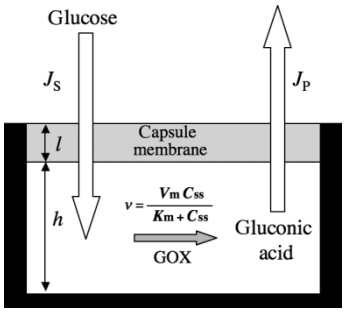

Figure 2. Schematic representation of the sensor response model.

Enzymatic reaction inside the sensing capsule

The enzymatic reaction inside the sensing capsule might follow the Michaelis–Menten kinetics

$$v = \frac{V_m C_{S(t)}}{K_m + C_{S(t)}}, \quad (2)$$

where v is the reaction velocity, K_m is the Michaelis constant and V_m is the maximum velocity.

The change in the glucose concentration inside the sensing capsule with time is given by subtracting the consumption rate of glucose due to the enzymatic reaction from glucose influx as

$$\frac{\partial C_{S(t)}}{\partial t} = \frac{J_{S(t)}}{h} - v, \quad (3)$$

where h is the effective thickness of the aqueous phase inside the sensing capsule.

Immediately after increasing the glucose concentration outside the sensing capsule, the influx of glucose becomes much larger than the velocity of the enzymatic reaction, reflecting lowered concentration of glucose inside the sensing capsule. In this case, the differential Equation (3) can be solved as

$$C_{S(t)} = C_S^0 + \left(C_{S(t=0)} - C_S^0\right)\exp\left[-\frac{D_S t}{hl}\right], \quad (4)$$

where $C_{S(t=0)}$ is the glucose concentration inside the sensing capsule at time zero.

When a steady state is reached between the influx of glucose and the enzyme reaction velocity, the following relation should be satisfied:

$$J_{S(t)} = hv. \quad (5)$$

The concentration of glucose inside the sensing capsule under a steady state, C_{SS}, and the time needed to reach a steady state after jumping the glucose concentration, T, can be described as

$$C_{SS} = \frac{1}{2}\left(C_S^0 - K_m - \frac{hlV_m}{D_S}\right) + \sqrt{C_S^0 K_m + \frac{\left(D_S\left(C_S^0 - K_m\right) - hlV_m\right)^2}{4D_S^2}}, \quad (6)$$

and

$$T = -\frac{hl}{D_S}\ln\left[\frac{C_{SS} - C_S^0}{C_{S(t=0)} - C_S^0}\right]. \quad (7)$$

Efflux of gluconic acid across the capsule membrane

When the concentration of gluconic acid outside the sensing capsule is negligible, the efflux of gluconic acid across the capsule membrane can be written as

$$J_{P(t)} = -D_P\frac{\partial C_P}{\partial x} = D_P\frac{C_{P(t)}}{l}, \quad (8)$$

where $J_{P(t)}$ is the efflux of gluconic acid at time t, D_P is the diffusivity of gluconic acid in the capsule membrane and $C_{P(t)}$ is the concentration of gluconic acid inside the sensing capsule.

The total concentration of gluconic acid, $Q^{tot}_{P(t)}$, generated by the enzymatic reaction can be described as

$$Q^{tot}_{P(t)} = \int_0^T \frac{V_m C_{S(t)}}{K_m + C_{S(t)}}dt + \int_T^t \frac{V_m C_{SS}}{K_m + C_{SS}}dt. \quad (9)$$

The remaining gluconic acid inside the sensing capsule, $C_{P(t)}$, can be obtained by the subtraction of the sum of the gluconic acid efflux from the total concentration of the generated gluconic acid

$$C_{P(t)} = Q^{tot}_{P(t)} - \frac{1}{h}\int J_{P(t)}dt. \quad (10)$$

Combination of Equations (8)–(10) leads to the following differential equation:

$$\frac{\partial Q^{tot}_{P(t)}}{\partial t} - \frac{\partial C_{P(t)}}{\partial t} = \frac{D_P}{hl}C_{P(t)}. \quad (11)$$

By solving Equation (11), the concentration of gluconic acid inside the sensing capsule, $C_{P(t)}$, can be obtained.

In the case of $t \geq T$, Equation (10) provides the following solution:

$$C_{P(t)} = \frac{hlV_mC_{SS}}{D_P(K_m + C_{SS})} + \left(C_{P(t=T)} - \frac{hlV_mC_{SS}}{D_P(K_m + C_{SS})}\right)\exp\left[-\frac{D_P(t-T)}{hl}\right], \quad (12)$$

where $C_{P(t=T)}$ is the concentration of gluconic acid inside the sensing capsule at time T. Consequently, the concentration of gluconic acid inside the sensing capsule under a steady state, C_{PS}, can be obtained with $t \to \infty$ as

$$C_{PS} = \frac{hlV_mC_{SS}}{D_P(K_m + C_{SS})}. \quad (13)$$

Simulations

The theoretical model described herein can be used to predict the sensor response and determine appropriate combinations of material properties and physical dimensions to achieve useful optical glucose-sensing capsules. A typical simulation approach is to generate a step increase in glucose concentration, C_S^0, at $t = 0$ and follows the resulting concentration of gluconic acid inside the sensing capsule, $C_{P(t)}$, as a function of time. The sensor response, i.e. the concentration of gluconic acid inside the sensing capsule, was calculated for a constant set of values; then diffusivity of gluconic acid, D_P, diffusivity of glucose, D_S, and effective thickness of the aqueous phase inside the sensing capsule, h, were varied systematically while holding the other values constant. Unless otherwise stated, the model used the following values: $D_S = 5.0 \times 10^{-8}\,cm^2\,s^{-1}$, $D_P = 5.0 \times 10^{-8}\,cm^2\,s^{-1}$, $K_m = 10\,mM$, $V_m = 10\,mM\,s^{-1}$, $C_S^0 = 0 - 5.0\,mM$, $l = 12\,\mu m$, $h = 50\,\mu m$. These constants were derived from either the experimental observations or the literature on GOX and diffusivities in polymeric membranes (*26–32*).

Results and discussion

Temporal response calculated by the proposed model

The surface plots in Figure 3 show the temporal distribution of gluconic acid inside the sensing capsule, which corresponds to a step increase in the concentration of bulk glucose. Figure 3(A) shows the plot of the concentration of gluconic acid, $C_{P(t)}$ vs. time and the concentration of bulk glucose, C_S^0, Figure 3(B) shows the plot of $C_{P(t)}$ vs. time and D_P, Figure 3(C) shows the plot of $C_{P(t)}$ vs. time and D_S and Figure 3(D) shows the plot of $C_{P(t)}$ vs. time and the effective thickness, h, of the aqueous phase inside the sensing capsule. The fundamental behaviour of the sensing capsules can be described from the analysis of these plots. The first item of note is the dependence of the concentration of bulk glucose on the temporal response. It has been found that the concentration of gluconic acid inside the sensing capsule is proportional to that of glucose in the bulk solution from 0 to 40 mM, reflecting Michaelis–Menten-type enzymatic kinetics; the concentration of gluconic acid reaches steady-state values within 10 min after jumping the glucose concentration (Figure 3(A)). With decreasing diffusivity of gluconic acid in the capsule membrane while holding that of glucose constant, a significant increase in the concentration of gluconic acid appears; when the diffusivity of gluconic acid is 10 times smaller than that of glucose, the concentration of gluconic acid in the sensing capsule becomes 10 times higher. Such an enrichment of the enzymatic product, achieved by regulating its diffusivity across the sensing capsule membrane, would be effective in the enhancement of sensor responses. The higher the enrichment of gluconic

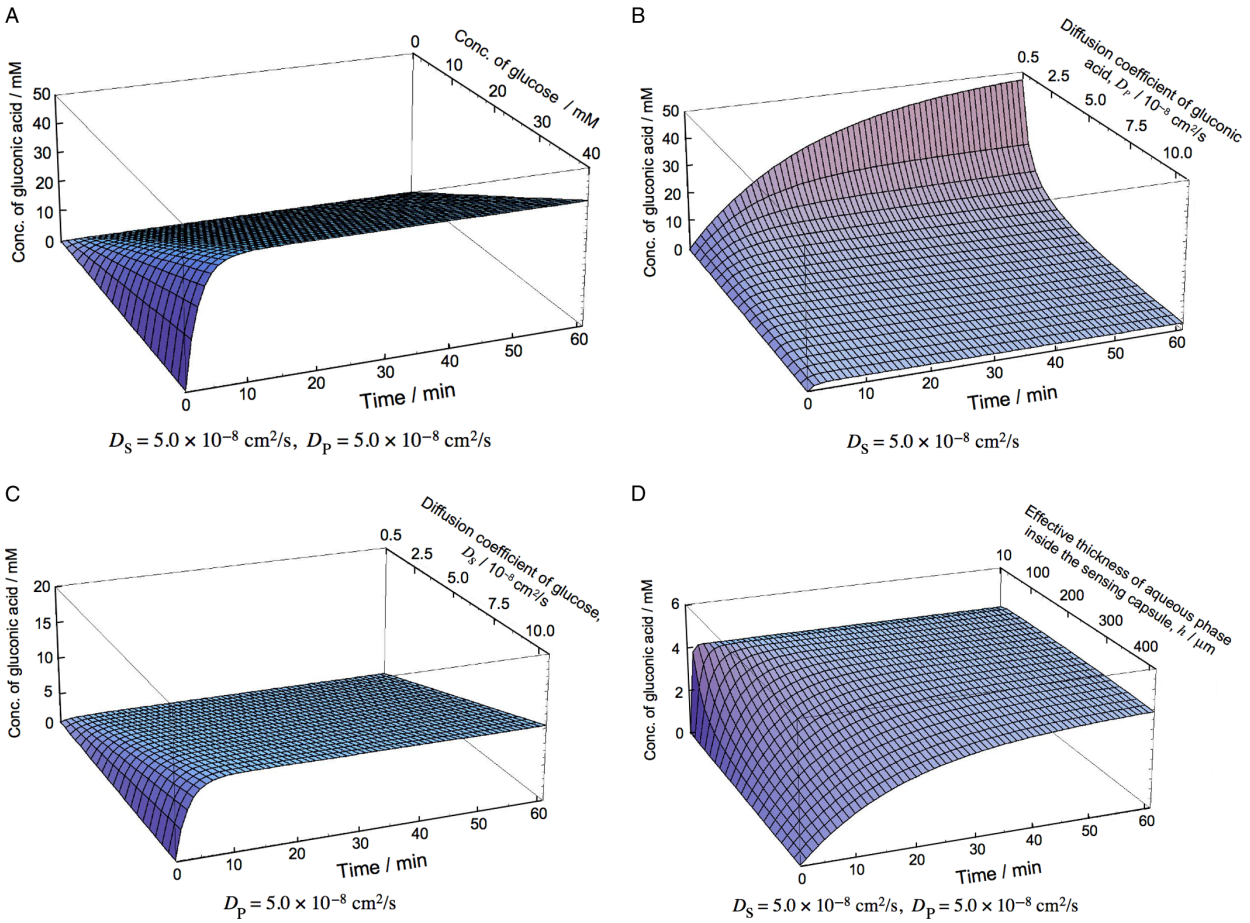

Figure 3. Surface plots of the temporal distribution of gluconic acid inside a sensing capsule, which corresponds to a step increase in the concentration of bulk glucose: (A) the concentration of gluconic acid $C_{P(t)}$ vs. time and the concentration of bulk glucose C_S^0; (B) $C_{P(t)}$ vs. time and D_P; (C) $C_{P(t)}$ vs. time and D_S; (D) $C_{P(t)}$ vs. time and the effective thickness, h, of the aqueous phase inside the sensing capsule. Unless otherwise stated, the model used the following values: $D_S = 5.0 \times 10^{-8}\,\mathrm{cm^2\,s^{-1}}$, $D_P = 5.0 \times 10^{-8}\,\mathrm{cm^2\,s^{-1}}$, $K_m = 10\,\mathrm{mM}$, $V_m = 10\,\mathrm{mMs^{-1}}$, $C_S^0 = 0 - 5.0\,\mathrm{mM}$, $l = 12\,\mu\mathrm{m}$ and $h = 50\,\mu\mathrm{m}$.

acid, however, considerably longer is the response time to reach its steady-state concentration (Figure 3(B)). On the other hand, the dependence of glucose diffusivity on the response time is not seen, whereas the steady-state concentration of gluconic acid increases with increasing diffusivity of glucose (Figure 3(C)). It is worth noting that the narrower effective thickness, h, of the sensing capsule as well as the thinner capsule membrane, l, (data not shown) makes the response time shorter, keeping the steady-state concentration of gluconic acid almost constant (Figure 3(D)). Such an effect on sensor dimension would provide precept for the fabrication of GOX-based optical sensors with fast and enhanced responses.

Glucose responses of optical-sensing capsules

A typical response of a sensing capsule for glucose in 10 mM PBS is shown in Figure 4. It can be seen that upon addition of glucose, the colour of the sensing capsule in the magnified image changes from orange to a bright bluish hue; the averaged red colour intensity of the image within the sensing capsule (taken every 60 min after changing the concentration of glucose) decreases with the increasing concentration of glucose. The bluish colour of the sensor in the presence of glucose indicates protonation of chromoionophore in pH/Na^+-sensing microscopic beads induced by a pH drop due to the enzymatic product, gluconic acid, inside the sensing capsule.

Optical pH-sensing beads could be based on several different principles, one of which could be the use of traditional dye molecules immobilised in or onto the beads. The colour change of such dyes cannot be tuned to match the specific application; however, one example is the classical pH dyes whose maximum sensitivity is at a fixed pH value, determined by the pK_a value of the dye. To optimise the colour response to glucose at physiologically relevant concentrations, 'tunable' dyes are a better choice. This can be obtained by adopting optode technology

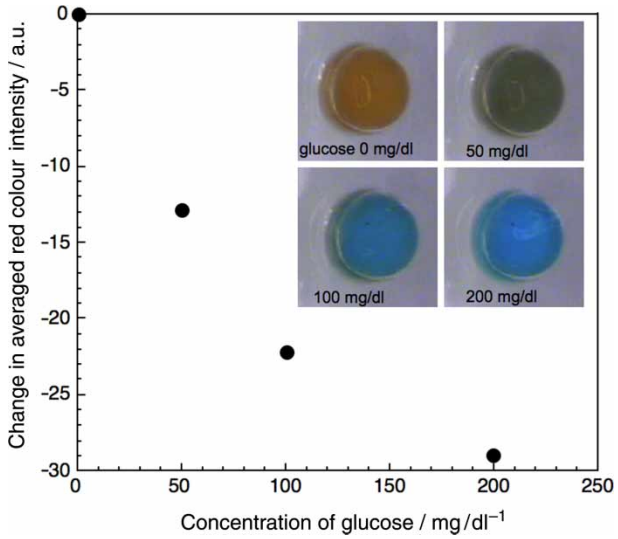

Figure 4. Typical response of a sensing capsule for glucose in a solution containing 10 mM PBS and the corresponding magnified sensor images (inset).

that is based on ion exchange between an aqueous sample and a lipophilic membrane loaded with an ionophore molecule that interacts with a suitable chromoionophore to produce colour change of the membrane: the dynamic range of the optode can be tuned to the respective concentration ranges of interest by changing the ratio of the ionophore and chromoionophore within the membrane (*24*, *25*).

A potential problem with optodes is that the colour depends on two species: H^+ and counter-cation. One of the solutions is to ensure the changes in pH due to glucose in the capsule are much greater than the ambient variations in pH and Na^+ concentration, such as in the relatively well-buffered interstitial fluid.

Effect of diffusivity of capsule membranes on glucose responses

The sensor capsule membranes with various diffusivities were successfully obtained by changing the monomer ratio between HEMA and PEGMA. Three kinds of sensors with different diffusivities of the capsule membranes but otherwise of the same composition were prepared: Sensors 1, 2 and 3 had capsule membranes prepared from a monomer mixture containing 90, 80 and 60 wt% of HEMA against the total weight of the monomers (HEMA + PEGMA), respectively (Table 1).

The typical time responses of optical-sensing capsules with various membrane diffusivities are shown in Figure 5(A), obtained by the jump in the concentration of glucose from 0 to 100 mg/dl. It was found that the shorter the response time for glucose, the higher is the content of PEGMA in the sensor capsule membrane; 90% of the response time for Sensor 3 with 40 wt% of PEGMA in the sensor capsule membrane was 10 min, whereas the red colour intensity of the time response for Sensor 1 with 10 wt% of PEGMA was still increasing with time after 30 min. On the other hand, the colour response of Sensor 1 was much greater than that of Sensor 3 with higher content of PEGMA in the capsule membrane.

In order to estimate the concentration of gluconic acid inside the sensing capsule, the observed red colour intensity of each sensor was initially converted to the local pH value inside the sensing capsule using pre-calibrated curves of the sensor colour intensity against the solution pH (Figure 5(B)). Such a conversion is reasonable because the local pH value inside the sensing capsule should be equal to the bulk solution pH in the absence of glucose. The concentration of gluconic acid inside the sensing capsule was then calculated from the corresponding pH value with a buffer capacity of 10 mM PBS and the dissociation constant of gluconic acid by assuming that the change in local pH would be mainly governed by the concentration of gluconic acid remaining inside the sensing capsule (Figure 6). The thus estimated concentrations of gluconic acid under steady state with diffusion were 6.0, 4.1 and 1.9 mM for Sensors 1, 2 and 3, respectively. It is worth noting that the concentration of gluconic acid for Sensor 1 was higher than that of glucose in the sample solution (5.6 mM), reflecting an enrichment of the enzymatic product by regulating its efflux from the sensing capsule.

Validation of the response model for sensing capsules with different diffusivities

The experimental time response for glucose as a function of the concentration of gluconic acid inside the sensing capsule was satisfactorily modelled by the developed theoretical approach, as shown in Figure 6. The solid line represents the theoretical curves obtained by fitting the data to the model Equations (6) and (12) with diffusion coefficients across the capsule membranes, D_S and D_P, as the variables. Good quality fit could be obtained for all sensors with particular values of diffusion coefficients, as summarised in Table 1.

It was found that the diffusion coefficient of gluconic acid, D_P, becomes smaller with increased content of HEMA in the capsule membrane, and follows the order Sensor 1 $\leq$ Sensor 2 $<$ Sensor 3. This might be due to a low affinity of anionic gluconate with HEMA-rich membranes. In fact, it was reported that the partition coefficient of negatively charged molecules with low molecular weight between water and poly-HEMA-based hydrogels is generally much smaller than that of positively charged ones (*29*). Additionally, it was also reported for poly(HEMA-co-PEGMA) hydrogels that the oxyethylene side chains on PEGMA offer the cross-linked polymer

Table 1. Diffusion coefficients of glucose and gluconic acid within the sensor capsule membranes obtained by the theoretical fitting of the data to the model Equations (6) and (12).

	Feed composition of capsule membrane (weight ratio)	Diffusion coefficient of glucose (D_S/cm^2 s^{-1})	Diffusion coefficient of gluconic acid (D_P/cm^2 s^{-1})
Sensor 1	HEMA/PEGMA = 9/1	3.8×10^{-8}	3.4×10^{-8}
Sensor 2	HEMA/PEGMA = 8/2	2.6×10^{-8}	3.5×10^{-8}
Sensor 3	HEMA/PEGMA = 6/4	2.2×10^{-8}	6.4×10^{-8}

chains more hydrogen-bonding sites with water; therefore, the water content of the gel increases as the PEGMA content increases (*29*). Such a water affinity of the PEGMA-rich capsule membrane might be another reason for the larger diffusivity of gluconic acid.

On the other hand, the largest glucose diffusivity was observed for Sensor 1 with the highest HEMA content in the capsule membrane. The formation of hydrogen bonds between dense hydroxyl groups of HEMA-rich membrane and uncharged glucose molecules might enhance the distribution of glucose into the capsule membrane.

Glucose diffusion coefficients in water, aqueous solutions, calcium alginate and agarose gel have been reported to be in the range of $6.1 - 9.2 \times 10^{-6}$ cm^2 s^{-1} (*30*). The reported glucose diffusion coefficients within the polymeric membranes decrease from polyether sulphone (5.7×10^{-6} cm^2 s^{-1}) (*31*) to polysulphone (2.8×10^{-6} cm^2 s^{-1}) (*31*) and polyvinyl alcohol (1.3×10^{-8} cm^2 s^{-1}) (*32*). Interestingly, the reported value of the glucose diffusion coefficient in an uncharged polyvinyl alcohol membrane having dense hydroxyl groups is comparable to that obtained in the capsule membranes, estimated using the proposed model for the sensor response function. This fact reinforces the usefulness of the model for predicting sensor responses. Direct measurements of diffusion coefficients of glucose and gluconic acid in poly(HEMA-co-PEGMA) membranes with a mass-transport cell for further validation of the proposed response model are currently under way.

Conclusions

A mathematical model for submillimetre-sized enzymatic optical-sensing capsules was derived, and the influence of permeability of the capsule membrane on the sensor response was studied. The model satisfactorily predicts the time responses of the enzymatic optical glucose-sensing capsules with various diffusivities and confirms that the regulation of the across-membrane diffusions of analyte (substrate) and the enzymatic product that induces the change in the sensor colour provides a significant enhancement of the sensor response.

It was found that the diffusivities of glucose and gluconic acid across the sensor capsule membrane were readily tuned by changing the monomer ratio between HEMA and PEGMA in the polymerisation process of sensor capsule membranes; a sensing capsule with

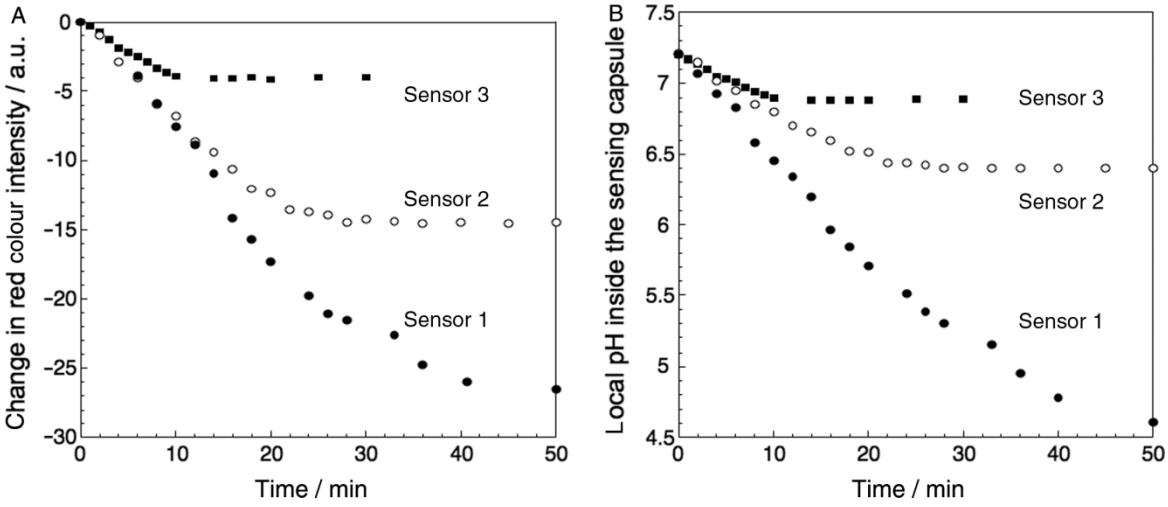

Figure 5. Time responses of the glucose-sensing capsules (Sensors 1, 2 and 3) obtained by a jump in the concentration of bulk glucose from 0 to 100 mg/dl in 10 mM PBS: (A) average red colour intensity of the corresponding sensor images and (B) local pH inside the sensing capsules vs. time.

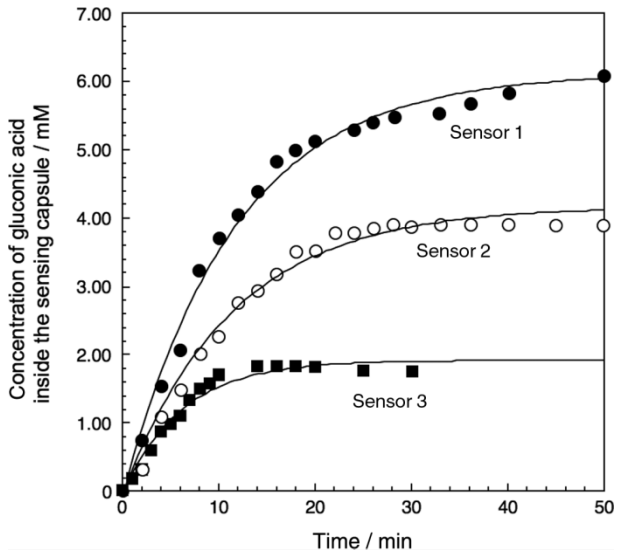

Figure 6. Time responses of the glucose-sensing capsules (Sensors 1, 2 and 3) as a function of concentration of gluconic acid inside the sensing capsules, obtained by a jump in the concentration of bulk glucose from 0 to 100 mg/dl in 10 mM PBS: (circles) estimated values from average red colour intensities of the corresponding sensor images; (solid lines) theoretical curves obtained by fitting the data to the model equations (6) and (12) with diffusion coefficients across the capsule membranes, D_S and D_P, as the variables.

a HEMA-rich membrane showed larger but slower glucose response, most likely due to low affinity of anionic gluconate with the HEMA-rich capsule membrane. Indeed, diffusion coefficients of gluconic acid (estimated on the basis of the proposed model) in the HEMA-rich capsule membranes were smaller than those in the PEGMA-rich capsule membranes.

The simplicity of the model facilitates prediction of the response function for enzymatic optical-sensing capsules and provides the following precepts for the design of the sensors with extremely enhanced responses: (1) increasing diffusivity of analyte across the capsule membrane, (2) decreasing diffusivity of enzymatic product, which induces sensor response, across the membrane and (3) reducing the volume inside the sensing capsule and the thickness of the capsule membrane to make the enhanced sensor response faster. We are currently fabricating submicrometre-sized enzymatic optical glucose-sensing capsules with rapid and extremely enhanced responses.

Acknowledgements

This work was supported by a Grant-in-Aid (No. 21550071) from the Japan Society of the Promotion of Science. Financial supports by NASA (Grant in Interdisciplinary Research and Technology in Support of Health-Related Countermeasures for Astronaut Crews) and partially by Vision Sensors LLC (Cleveland, OH, USA) are gratefully acknowledged.

References

(1) Heller, A.; Feldman, B. *Chem. Rev.* **2008**, *108*, 2482–2505.
(2) Sieg, A.; Guy, R.H.; Begona Delgado-Charro, M. *Diabetes Technol. Ther.* **2005**, *7*, 174–197.
(3) McNichols, R.J.; Cote, G.L. *J. Biomed. Opt.* **2000**, *5*, 5–16.
(4) Heinemann, L. *Diabetes Res. Clin. Pract.* **2006**, *74*, S82–92.
(5) Laird, T.; Zisser, H.; Jovanovic, L. *Diabetes Technol. Ther.* **2008**, *10*, S82–88.
(6) Wang, J. *Talanta* **2008**, *75*, 636–641.
(7) Kondepati, V.R.; Heise, H.M. *Anal. Bioanal. Chem.* **2007**, *388*, 545–563.
(8) Mahoney, J.; Ellison, J. *Clin. Chem.* **2007**, *53*, 1122–1128.
(9) Pickup, J.C.; Hussain, F.; Evans, N.D.; Sachedina, N. *Biosens. Bioelectron.* **2005**, *20*, 1897–1902.
(10) Wilson, G.S.; Hu, Y. *Chem. Rev.* **2000**, *100*, 2693–2704.
(11) Albers, J.; Grunwald, T.; Nebling, E.; Piechotta, G.; Hintsche, R. *Anal. Bioanal. Chem.* **2003**, *377*, 521–527.
(12) Gooding, J.J.; Hall, E.A.H. *J. Electroanal. Chem.* **1996**, *417*, 25–33.
(13) Katz, E.; Heleg-Shabtai, V.; Willner, B.; Willner, I.; Bückmenn, A.F. *Bioelectrochem. Bioenerg.* **1997**, *42*, 95–104.
(14) Gooding, J.J.; Hall, E.A.H.; Hibbert, D.B. *Electroanalysis* **1998**, *10*, 1130–1136.
(15) Ivanauskas, F.; Kaunietis, I.; Laurinavicius, V.; Razumiene, J.; Simkus, R. *J. Math. Chem.* **2005**, *38*, 355–366.
(16) Katz, E.; Willner, I. *Electroanalysis* **2005**, *17*, 1616–1626.
(17) Mackey, D.; Killard, A.J.; Ambrosi, A.; Smyth, M.R. *Sens. Actuators B* **2007**, *122*, 395–402.
(18) Masson, J.-F.; Kranz, C.; Booksh, K.S.; Mizaikoff, B. *Biosens. Bioelectron*. **2007**, *23*, 355–361.
(19) Kottke, P.A.; Kranz, C.; Kwon, Y.K.; Masson, J.-F.; Mizaikoff, B.; Fedorov, A.G. *J. Electroanal. Chem.* **2008**, *618*, 74–82.
(20) Brown, J.Q.; McShane, M.J. *Biosens. Bioelectron*. **2006**, *21*, 1760–1769.
(21) Stein, E.W.; Grant, P.S.; Zhu, H.; McShane, M.J. *Anal. Chem.* **2007**, *79*, 1339–1348.
(22) Stein, E.W.; Singh, S.; McShane, M.J. *Anal. Chem.* **2008**, *80*, 1408–1417.
(23) Tohda, K.; Gratzl, M. *Chem. Phys. Chem.* **2003**, *4*, 155–160.
(24) Tohda, K.; Gratzl, M. *Anal. Sci.* **2006**, *22*, 383–388.
(25) Tohda, K.; Gratzl, M. *Anal. Sci.* **2006**, *22*, 937–941.
(26) Liu, Y.; Wu, S.; Ju, H.; Xu, L. *Electroanalysis* **2007**, *19*, 986–992.
(27) Karmali, K.; Karmali, A.; Teixeira, A.; Curto, M.; Marcelo, M.J. *Anal. Biochem.* **2004**, *333*, 320–327.
(28) Kermis, H.R.; Rao, G.; Barbari, T.A. *J. Membr. Sci.* **2003**, *212*, 75–86.
(29) Lee, W.-F.; Lin, W.-J. *J. Polym. Res.* **2003**, *10*, 31–38.
(30) Rong, Z.; Cheema, U.; Vadgama, P. *Analyst* **2006**, *131*, 816–821.
(31) Crucio, E.; Bartolo, L.D.; Barbieri, G.; Renda, M.; Giorono, L.; Morelli, S.; Drioli, E. *J. Biotech.* **2005**, *117*, 309–321.
(32) Phanthong, C.; Somasundrum, M. *J. Electroanal. Chem.* **2003**, *558*, 1–8.